Chemistry–A European Journal
Research Article
doi.org/10.1002/chem.202303631
Chemistry Europe
European Chemical Societies Publishing
www.chemeurj.org

Targeting the Antifungal Activity of Carbon Dots against *Candida albicans* Biofilm Formation by Tailoring Their Surface Functional Groups

Elisa Sturabotti,*[a] Alessandro Camilli,[a] Vyali Georgian Moldoveanu,[a] Graziana Bonincontro,[b] Giovanna Simonetti,[b] Alessio Valletta,[b] Ilaria Serangeli,[c] Elena Miranda,[c] Francesco Amato,[a] Andrea Giacomo Marrani,[a] Luisa Maria Migneco,[a] Simona Sennato,[d] Beatrice Simonis,[a, e] Fabrizio Vetica,*[a] and Francesca Leonelli*[a]

Carbon dots (CDs) are an emerging class of carbon nanoparticles, which for their characteristics have found applications in many fields such as catalysis, materials and biomedicine. Within this context, the application of CDs as antibacterial agents has received much attention in very recent years, while their use as antifungal nanoparticles has been scarcely investigated. Here we report a systematic investigation of the surface functional groups of CDs to study their influence on these nanoparticles' against *Candida albicans*. Three classes of CDs have been synthesised and fully characterized. A thorough *in vitro* and *in vivo* biological screening against *C. albicans* was performed to test their antifungal, antiadhesion and antibiofilm formation activities. Moreover, the interaction with *C. albicans* cells was investigated by microscopic analysis. Our results evidence how the presence of a positively polarised surface results crucial for the internalization into COS-7 cells. Positively charged nanoparticles were also able to inhibit adhesion and biofilm formation, to interact with the cellular membrane of *C. albicans*, and to increase the survival of *G. mellonella* infected larvae after the injection with positive nanoparticles. The antifungal activity of CDs and their extremely low toxicity may represent a new strategy to combat infections sustained by *C.albicans*.

Introduction

Carbon dots (CDs) are an emerging class of carbon nanoparticles (up to 10 nm in diameter), possessing a plethora of peculiar properties such as biocompatibility, low toxicity, photoluminescence and photostability, and good suspensibility in water and organic solvents.[1] These quasi-spherical particles are prepared *via* two main synthetic approaches, *bottom-up* or *top-down*, by different technical procedures: hydrothermal, microwave-assisted as well as electrochemical.[2] The two approaches involve the use either of small organic compounds such as amino acids, carbohydrates and many more (*bottom-up*) as substrates or by exfoliation of larger carbon sources such as graphene, graphite or even biomass waste (*top-down*).[3]

From a structural point of view, the choice of the synthetic approach and, more importantly, of the starting material for the preparation of CDs is crucial to exert the desired application. In fact, the *bottom-up* methodology, which provides higher versatility in the preparation of functional nanomaterials, relies on the polymerization/dehydration of organic compounds, accreting the nanostructures until the energy source is stopped. Due to this synthetic mechanism, the active surface of the nanodots retains the structure and functional groups of the substrates. Typically, amino acids or citric acid are the popular choices as CDs precursors, leading mainly to –COOH, –OH, or

[a] Dr. E. Sturabotti, A. Camilli, V. Georgian Moldoveanu, Dr. F. Amato, Prof. Dr. A. Giacomo Marrani, Dr. L. M. Migneco, Dr. B. Simonis, Dr. F. Vetica, Prof. Dr. F. Leonelli
Department of Chemistry, Sapienza University of Rome, Piazzale Aldo Moro 5, 00185 Rome, Italy, URL:
and
Center for Cooperative Research in Biomaterials (CIC biomaGUNE), Paseo de Miramón 194, Donostia-San Sebastián 20014, Spain,
E-mail: fabrizio.vetica@uniroma1.it
francesca.leonelli@uniroma1.it
elisa.sturabotti@uniroma1.it
esturabotti@cicbiomagune.es
Homepage: https://www.chem.uniroma1.it/en/department/people/francesca-leonelli
https://www.chem.uniroma1.it/en/department/people/fabrizio-vetica
[b] G. Bonincontro, Prof. Dr. G. Simonetti, Prof. Dr. A. Valletta
Department of Environmental Biology, Sapienza University of Rome, Piazzale Aldo Moro 5, 00185 Rome, Italy
[c] Dr. I. Serangeli, Prof. Dr. E. Miranda
Department of Biology and Biotechnologies "Charles Darwin", Sapienza University of Rome, Piazzale Aldo Moro 5, 00185 Rome, Italy
[d] Dr. S. Sennato
CNR-Institute of Complex Systems (ISC)- Sede Sapienza c/o Physics Department, Sapienza University, Piazzale Aldo Moro 5, Rome, Italy
[e] Dr. B. Simonis
Institute for Biological Systems (ISB), Italian National Research Council (CNR), Sede secondaria di Roma – Meccanismi di Reazione, c/o Dipartimento di Chimica, Piazzale Aldo Moro 5, 00185 Rome, Italy

Supporting information for this article is available on the WWW under https://doi.org/10.1002/chem.202303631

$-NH_2$ decorated surfaces. Nevertheless, it has been reported that a careful selection of the organic precursors can lead to a fine tailoring of the active surface, depending on the envisioned nanomaterial purposes.[4]

For their extensive structural versatility, CDs have been employed in many research fields, such as biomedicine,[1d,5] agriculture,[6] and catalysis.[7] Within the former, the application as antimicrobial agents or as nanocarriers for antimicrobial drugs,[8] mainly antibacterial,[8b,9] have been studied over the last ten years. It has been demonstrated that positive polarization of the CDs surface, by introduction of amine/ammonium salt groups, is crucial for the antibacterial activity, which is ascribed to a better interaction with the negatively charged bacterial membranes, exerting the bactericidal and bacteriostatic actions *via* multiple routes: physical and mechanical damages to the bacterial membrane, or internalization followed by photo-activated generation of ROS and/or DNA or protein damage.[10] Hence, it appears clear that fine-tuning of surface functional groups of bioactive CDs is crucial for their antimicrobial targeting.

While the antibacterial application of CDs has been largely investigated and the surface/antibacterial relation has been thoroughly studied, the test of their antifungal properties has been scarcely reported. To the best of our knowledge, only two works report the direct *in vitro* antifungal application of CDs,[9c,11] one of which uses commercially available CDs.[11] Furthermore, the screening activity of CDs on procaryotic microorganisms is carried out using mostly the diffusion disk assay, without going into the details of fungi biofilm formation, adhesion and *in vivo* cytotoxicity. Consequently, a systematic screening of the required molecular features to produce effective antifungal carbon nanodots, together with a preliminary assessment of their anti-biofilm activity could be of crucial importance.

Nowadays, the landscape of fungal resistance and invasive fungal infection is dramatically changing,[12] highlighting the need to find new antifungal agents, especially targeting fungal adhesion and biofilm formation.[13] Within this context and due to our interests in organic synthesis and evaluation of antifungal compounds,[14] and more recently on CDs chemistry,[2a,7c,i] we envisioned the possibility to test the antifungal activity of microwave-synthesized CDs, still scarcely explored. Hence, we selected *C. albicans* as model target for our preliminary investigation of different classes of CDs, systematically screening how polarisation of the active surface can influence their eventual antifungal activity in *in vitro* and *in vivo* experiments (Figure 1). The selection of *C. albicans* as model target lies on its tendency to form biofilms, which express strong resistivity to conventional antifungal drugs, causing severe and acute medical infections. In the present work, three classes of CDs were prepared, possessing differently composition and charged surfaces, which were completely characterised with regards to their morphology and physicochemical properties. We demonstrate the requirement of a positively-charged

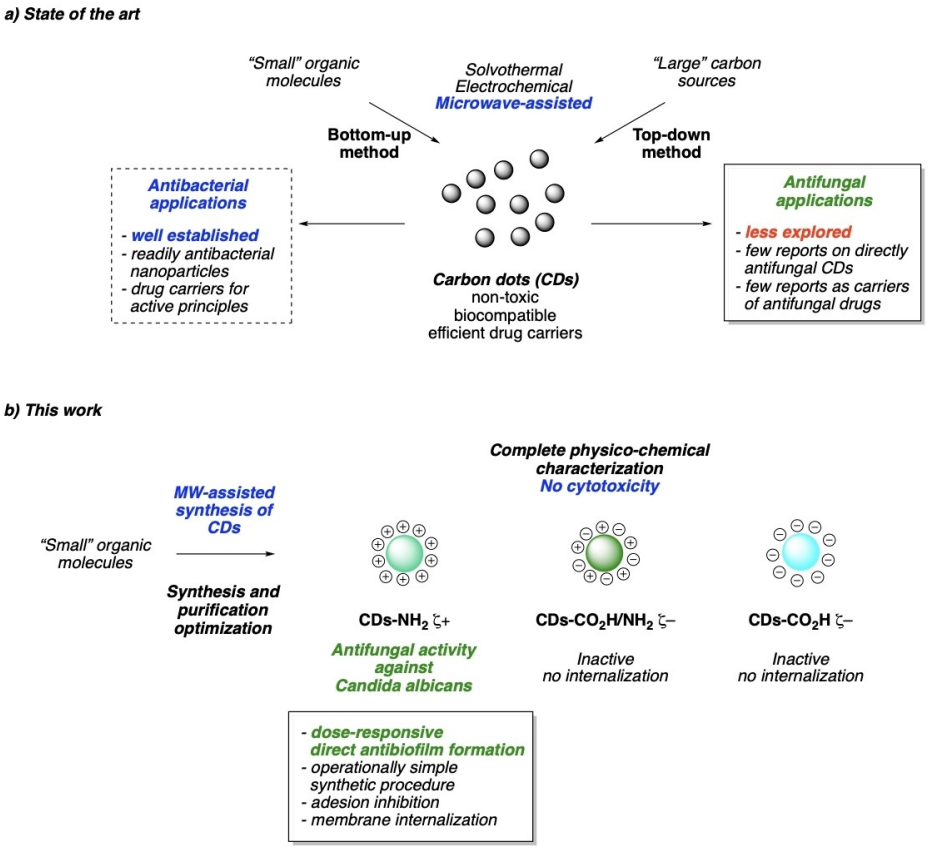

Figure 1. Schematic representation of the state of the art of antimicrobial carbon dots (a) and this current work (b).

surface on CDs to exert antibiofilm formation by *C. albicans*, highlighting a good dose-responsive activity, paired with anti-adhesion and internalization properties, and with a mortality reduction of infected larvae in *in vivo* tests. Moreover, low cytotoxicity of CDs towards fibroblast-like mammalian cells and *G. mellonella* larvae was demonstrated.

Results and discussion

Our investigation started with the synthesis of CDs from various carbon sources, for the initial screening and evaluation of their possible antifungal activity. We relied on a bottom-up microwave-assisted approach, changing the starting material to achieve different functional groups on the active surface of the nanoparticles. Three sets of CDs were prepared as depicted in Scheme 1. The first set of CDs was selected due to the extensive amine-rich active surface, and were prepared starting from D-glucosamine HCl (**1**) and 1,3-diaminobenzene (**2**) (Scheme 1a). Our synthetic strategy was based on literature procedures,[15] modifying the reaction time, wattage, and purification steps. A mixture of **1** and **2** in a 1:1.1 ratio was solubilized in a water/MeOH mixture (2:1) and carbonised in a microwave oven at 800 W for 3 min. The reaction time and MW wattage were optimized and set at these values in order to have reproducible results in terms of yield, dimensions and fluorescence properties of the CDs. In fact, by lowering the power to 600 MW or the time to 2 min we failed to produce the desired nanoparticles, while increasing the time led to larger and polydisperse CDs. The resulting slurry solution was diluted in water (10 mL), centrifuged at 4,000 rpm to remove larger particles and the supernatant was directly dialysed for five days and then filtered through a 100 nm syringe filter. The resulting solution was freeze-dried to obtain the desired CDs, namely **CDs**–$\mathbf{NH_2}$.

The size of **CDs**–$\mathbf{NH_2}$ was analysed comparing results from atomic force microscopy (AFM) and dynamic light scattering (DLS) measurements in dry and wet conditions, respectively. The nanoparticles obtained exhibited a monodisperse dimension with an average size of 2.022 ± 0.064 nm, as determined by analysis of height distribution calculated by AFM images. NNLS number-weighted analysis of DLS measurements showed a mean hydrodynamic diameter of 4.9 nm, larger than AFM determination, as expected due to hydration of CDs. Surface charge of carbon nanodots was investigated by means of zeta potential measurements in Milli-Q water, confirming that microwave assisted synthesis of CDs with amino-rich precursors resulted in the formation of positive-charged nanoparticles ($+14.3 +/- 0.21$ mV, Figure 2b and Figure S7 in the Supporting Information (SI), respectively). Besides the morphological and surface charge characterization of CDs, the composition of the nanoparticles is strongly related to their physico-chemical and biological features and therefore it should be rigorously assessed. Accordingly, X-ray photoelectron spectroscopy (XPS), Fourier-transform infrared spectroscopy in attenuated total reflection mode (ATR-FTIR) and elemental analysis were combined to elucidate in detail the chemical content of the **CDs**–$\mathbf{NH_2}$. The XPS spectrum of C 1s region revealed the presence of an aromatic carbon core decorated with aminic and oxygenated (mainly hydroxyls) functional groups (Figure 2c, upper panel). The presence of ammonium groups was ascertained in the N 1s region (Figure 2c, lower panel), where the component at 402 eV can be assigned to positively charged

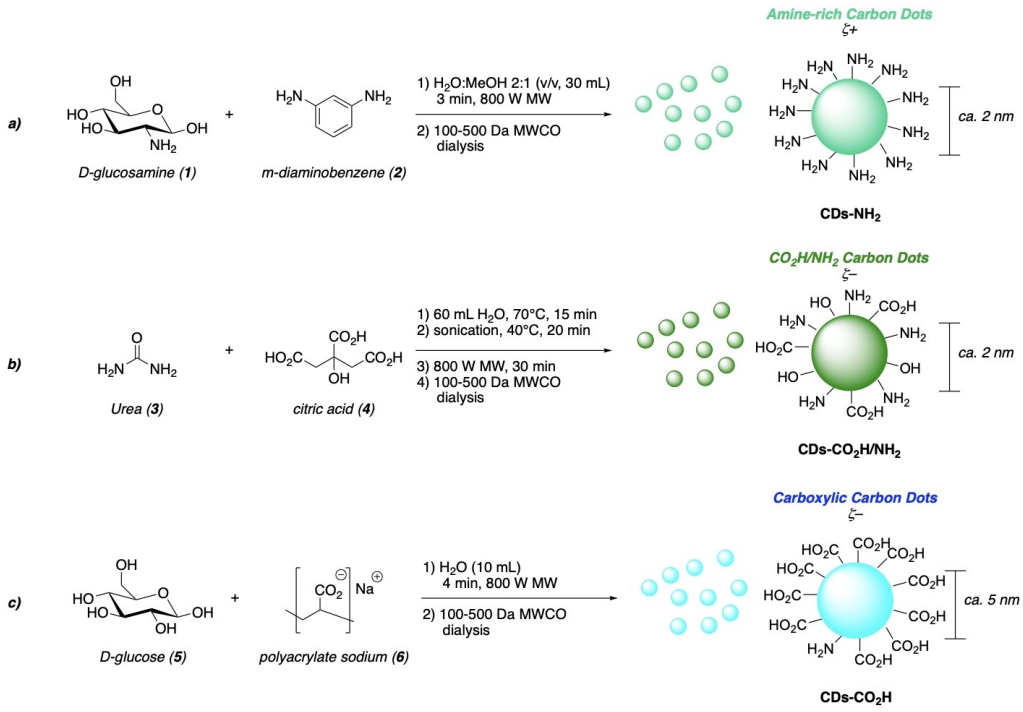

Scheme 1. Synthesis of three different sets of CDs, varying the active surface functional groups.

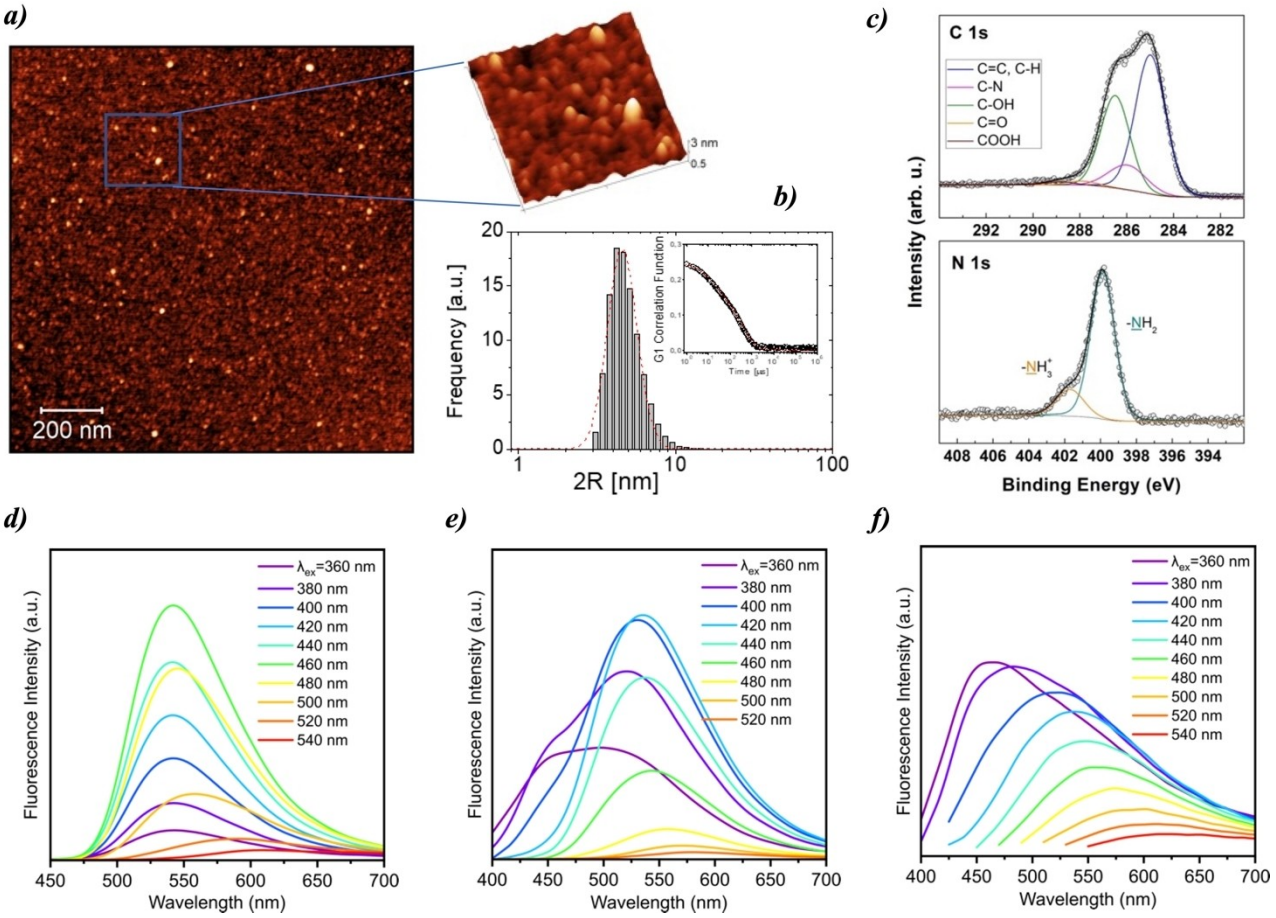

Figure 2. Characterization images and spectra of the synthesized CDs. a) AFM image (height sensor) of **CDs**–$\mathbf{NH_2}$; b) DLS number-weighted size distribution of **CDs**–$\mathbf{NH_2}$, with the measured DLS G1 correlation function shown in the inset; c) XPS C 1s (upper) and N 1s (lower) spectra of **CDs**–$\mathbf{NH_2}$; d) fluorescence spectra of **CDs**–$\mathbf{NH_2}$; e) fluorescence spectra of **CDs**–$\mathbf{CO_2H/NH_2}$; f) fluorescence spectra of **CDs**–$\mathbf{CO_2H}$.

N atoms, compensated by residual Cl^- anions (see Cl 2p spectrum, Figure S12 Supporting Information). Presence of nitrogen and oxygen-containing groups onto CDs was further confirmed by ATR-FTIR spectra analysis (Figure S21). In fact, the spectrum of **CDs**–$\mathbf{NH_2}$ displays specifics absorption bands centred at 3320 and 3210 cm^{-1} for N–H and O–H stretching, 1620 and 1500 cm^{-1} for amides stretching and 1070 cm^{-1} for C–N bond stretching. The amount of carbon, hydrogen and nitrogen in the purified **CDs**–$\mathbf{NH_2}$, express as weight percentage, was measured by elemental analyses experiments (Table S3 in SI). Positively-charged N-doped carbon dots were characterized by a carbon to nitrogen ratio of 4:1. The UV-vis spectrum of **CDs**–$\mathbf{NH_2}$ highlighted an intense absorption at 218 nm, relative to the π-π* transitions of the aromatic core, and a lower absorption centred at 370 nm ascribable to the n-π* transitions of C=C, C=O and C=N double bonds (Figure S22, SI). Furthermore, the fluorescence analysis showed a bright green centred emission at 530 nm, independent by the excitation wavelength ($\lambda^{em}_{max} = 460$ nm), indicating a uniform emissive core.

For the second set of CDs, classically used starting materials were selected: urea (**3**) and citric acid (**4**) (Scheme 1b).[16] These substrates would indeed lead to the presence of both amino and carboxyl functionalities and a resulting neutrally charged surface. The substrates were dissolved in water at 70 °C for 15 min, followed by 20 min sonication to ensure complete solubilization. Then, the solution was irradiated at 800 W for 30 min, followed by the same purification steps previously described. The obtained CDs, namely **CDs**–$\mathbf{CO_2H/NH_2}$, were isolated and fully characterized (characterisation data in the SI). **CDs**–$\mathbf{CO_2H/NH_2}$ showed nanoparticles with an average size of 2 nm determined by analysis of AFM height profile and a mean hydrodynamic diameter of 60 nm obtained by NNLS number-weighted analysis of DLS data. Interestingly, the ζ potential analysis evidenced an overall negative charge of the surface (−22 mV), reasonably due to co-presence of aminic and carboxyl groups with a slight excess of the latter, which was verified by XPS and FTIR analyses. Specifically, The C 1s XPS spectrum (Figure S14, SI) showed the presence of a mixture of functional groups appended to the aromatic carbon core, including amines, hydroxyls, carboxylates and carboxylic moieties. The N 1s region (Figure S15, SI) confirmed the presence of aminic groups with a small fraction of ammonium. The presence of peaks at 1700 cm^{-1} and 1550 cm^{-1} in IR spectrum indicated the stretching of carboxylic and carboxylate groups, while the peaks at 3210 cm^{-1} and 1070 cm^{-1} were ascribable at

N–H and C–N stretching, respectively. The spectrofluorimetric study revealed slightly different results compared to literature data,[16] reasonably because of the variation in the power used for CDs synthesis, displaying emission-dependent bright-green fluorescence emission, centred at 539 nm (Figure 2e),

Subsequently, we focused on the synthesis on the third set of carbon dots, possessing a negatively charged surface and without N-doping. In this case, modifying a literature procedure (see SI for the screening of reaction conditions and optimization),[17] we selected D-glucose (**5**) and polyacrylate sodium (MW = 5100, **6**), in a 1:2 ratio, as starting materials (Scheme 1c). The microwave-assisted carbonisation was performed in water, irradiating for 4 min at 800 W, followed by the previously optimized purification.

These newly synthesized nanoparticles were also completely characterized (characterisation data in the SI). The negative zeta potential was confirmed by DLS analysis (-36.23 ± 0.78 mV), together with an average hydrodynamic diameter of around 5 nm, as determined by NNLS number-weighted DLS analysis. The morphology analysis by AFM showed quasi-spherical CDs of average height around 1.3 nm, determined by analysis of height profile. The C 1s XPS spectrum (Figure S18, SI) revealed the presence of both COOH and carboxylate functional groups, as expected from the use of sodium polyacrylate, with the addition –OH moieties. The presence of Na^+ was confirmed in the Na 1s region (Figure S19, SI). The fluorescence analysis highlighted also in this case an excitation-dependent emission, with a maximum emission centered at 450 nm ($\lambda^{em}_{max} = 480$ nm, Figure 2f). The negatively charged surface was ascribable to carboxyl moieties, as also confirmed by XPS and by the presence in the FTIR spectrum of peaks at 1700 cm^{-1} and 1550 cm^{-1} (O–H and C=O stretching, respectively).

Carbon dots have attired much attention by the scientific community due to their biocompatibility and for their variety of biological applications. To check if biocompatibility was retained by the envisioned classes of carbon nanodots in hand, we conducted preliminary cytotoxicity test on COS-7 cells, a fibroblast-like mammalian cell line derived from monkey kidney tissue, using the MTT (3-(4,5-dimethylthiazol-2-yl)- 2,5-diphenyl-tetrazolium bromide) assay to assess cell viability after 48 h of exposure. In this assay, the MTT salt is reduced to purple formazan crystals by mitochondrial dehydrogenases active in the healthy cells. The amount of formazan produced is proportional to the number of viable cells in the culture and can be measured spectrophotometrically. COS-7 cells were treated with various concentrations of each type of CDs, ranging from 0.125 up to 4 mg/mL and the results are shown in Figure 3. At all tested concentrations, the cell viability was extremely high. In particular, **CDs–NH_2** and **CDs–CO_2H/NH_2** exhibit negligible cytotoxicity against COS-7 cells for all the investigated concentrations. Only the **CDs–CO_2H** shows a concentration-dependant behaviour, causing a decrease in cell viability starting from 1 mg/mL up to 4 mg/mL when treated for 48 h. In addition to the MTT assay, a Trypan blue exclusion assay showed that most of the COS-7 cells were attached to the plate (no cells were found in the culture medium supernatant) and most of them were live (Supplementary Figure 23).

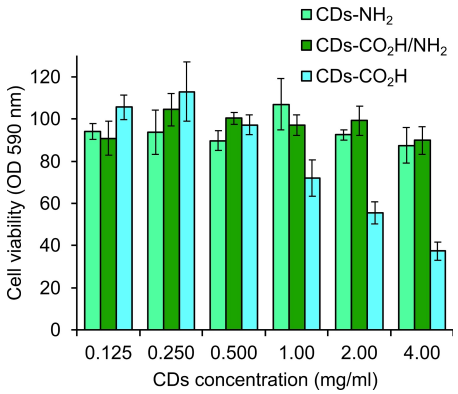

Figure 3. Cell viability MTT assay of cultured cells treated with **CDs–NH_2**, **CDs–CO_2H/NH_2**, **CDs–CO_2H** for 48 h. All experiments were performed at least 3 times. No significant differences were observed with ANOVA statistical analysis.

To understand if carbon dots were able to pass through the cell membrane, and did not accumulate on the cell surface, we used live cell confocal microscopy (λ_{exit} 450–490 nm; λ_{flu} 515 nm) that produces a resolved image of a single focal plane, without disturbance from other regions of the cell. Importantly, no signal was observed when the cells were treated with **CDs–CO_2H/NH_2** and **CDs–CO_2H**, while a strong green signal, ascribable to the dots fluorescence, was visible in cells treated with **CDs–NH_2** (Figure 7, a and b), underlying the possibility to use **CDs–NH_2** as imaging probe for biological fluorescent imaging. We observed that **CDs–NH_2** signal is visible inside the cell, suggesting that this compound is able to permeate the mammalian cell membrane (Figure 7, c). This crucial result highlights that the main structural feature of the surface that is necessary for cellular internalization is not related only to the functional groups and general elemental composition but to the total surface polarization, which plays a pivotal role in the establishment of electrostatic interaction with the cell membrane. Indeed, while **CDs–NH_2** are characterized by aminic groups and a positively polarized surface, **CDs–CO_2H/NH_2** also present aminic moieties, however the total surface charge is negative. The capacity of **CDs–NH_2** to be internalized while maintaining extremely high viability are promising features for the envisioned antimicrobial applications of these nanomaterials in the biomedical field.

Prompted by these encouraging results, we extended our study to the evaluation of the CDs antifungal activity, selecting *C. albicans* as biological target, due to its relevant healthcare role. The broth microdilution method has been performed to evaluate CDs antifungal activity against *C. albicans* planktonic cells, following CLSI standard methods.[18] The results reported in Table S5 (SI) showed that **CDs–NH_2** had the best activity with MIC value, expressed as Geometric Mean (GM), of 397 μg/mL, while **CDs–CO_2H/NH_2** and **CDs–CO_2H** had no activity at the highest concentration (500 μg/mL). The results obtained with the reference compounds fluconazole and amphotericin B (literature values) highlight that **CDs–NH_2** showed a low capacity to inhibit *C. albicans* planktonic cells. Nevertheless, the major concerns about *C. albicans* infections, as above stated, is

its tendency to form biofilm, which dramatically increase resistance to antimicrobials and immune cells.

Adhesion and biofilm formation by *C. albicans* are important virulence factors and new antifungal therapies aim to inhibit them, to prevent the establishment of hard-to-treat infections.[19] *C. albicans* is able to adhere to both biotic and abiotic surfaces, causing colonization which can lead to invasive infections. For this reason, CDs' anti-*Candida* adhesion assay was performed on flat-bottomed, 48-well microtiter plates, as previously described[20] with some modifications. The three sets of CDs showed the capacity to inhibit *C. albicans* adhesion to polystyrene microtiter plates in a dose-dependent manner (Figure 4). Positive surface charged CDs (**CDs**–$\mathbf{NH_2}$) showed a significant activity when compared with **CDs**–$\mathbf{CO_2H/NH_2}$ and **CDs**–$\mathbf{CO_2H}$ (p value <0.001). **CDs**–$\mathbf{NH_2}$ reduce *C. albicans* adhesion by 79% at a concentration of 500 μg/mL, after 90 minutes of incubation.

C. albicans adhesion is followed by biofilm formation on the colonized surface. During biofilm formation, cells organize in a community and start to secrete the extracellular matrix (ECM), which is the main responsible for the higher resistance of biofilms to antifungal drugs. CDs activity was investigated *in vitro* against *C. albicans* biofilm formation, using flat-bottomed, 48-well microtiter plates, as previously described.[19b,21] CDs at a concentration ranging from 500 μg/mL to 0.976 μg/mL were used for these experiments. The three sets of CDs showed the capacity to inhibit biofilm formation in a dose-dependent manner (Figure 5). Again, the positive surface charged **CDs**–$\mathbf{NH_2}$ showed a significant inhibition activity against *C. albicans* earlier (24 h) and mature biofilm (48 h) (p value <0.001) when compared with **CDs**–$\mathbf{CO_2H/NH_2}$ and **CDs**–$\mathbf{CO_2H}$. In particular, **CDs**–$\mathbf{NH_2}$, at the concentration of 500 μg/mL, reduced biofilm formation by 89% and 95%, respectively, after 24 h and 48 h. For the **CDs**–$\mathbf{NH_2}$, good results in terms of anti-biofilm activity were visible yet from 125 μg/mL since more that 70% of earlier and mature biofilm is inhibited.

In recent years, *G. mellonella* larvae have been widely used to test the antimicrobial activity of both chemical and natural compounds *in vivo* due to the remarkably mammalian-like immune system. In addition, this animal model meets the bioethics principle of the 3Rs (Replacement, Reduction, and Refinement) in animal experimentation and is characterized by

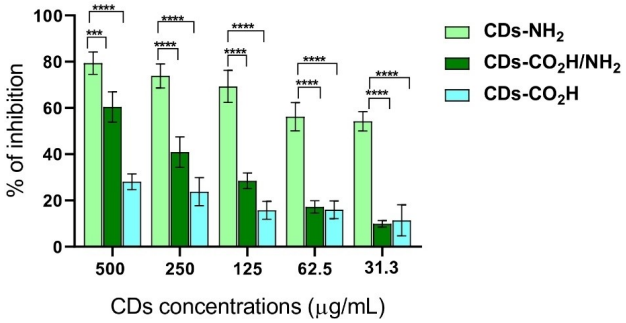

Figure 4. Inhibition of *C. albicans* ATCC 10231 adhesion to polystyrene wells in the presence of **CDs**–$\mathbf{NH_2}$ (lime green), **CDs**–$\mathbf{CO_2H/NH_2}$ (green), **CDs**–$\mathbf{CO_2H}$ (blue) after 90 min.

simple handling and experimental procedures.[22] Hence, the in vivo antifungal activity evaluation of **CDs**–$\mathbf{NH_2}$ was carried out treating pre-infected *G. mellonella* with **CDs**–$\mathbf{NH_2}$ at different concentration and evaluating the amount of survival larvae after 120 h (procedure in the SI).[14d] Three control groups were defined: untreated larvae, larvae injected with PBS and larvae infected with *C. albicans*. Three groups of infected larvae were then treated with different concentrations of **CDs**–$\mathbf{NH_2}$: 5000 μg/mL, 500 μg/mL, 50 μg/mL (Figure 6). No mortality was recorded among untreated larvae and larvae injected with PBS. The mortality rate of the infected G. mellonella larvae was 20%. When compared with the control, **CDs**–$\mathbf{NH_2}$ 5000 μg/mL and 500 μg/mL showed significant results (p value <0.01, p value <0.05, respectively). Larvae survival increases by up to 90% following treatment with the highest concentration tested, 5000 μg/mL (Figure 6, a), and by up to 80% after injection with 500 μg/mL (Figure 6, b), showing interesting dose-dependent behaviour of **CDs**–$\mathbf{NH_2}$ even in *in vivo* tests (active concentration below COS-7 MTT results), Figure 7.

By exploiting the intrinsic fluorescence of CDs and encouraged by the internalization results obtained on COS-7 cells, epifluorescence microscopy was employed to investigate the internalization of CDs in planktonic and biofilm-associated *Candida albicans* cells. No fluorescent signal was observed in **CDs**–$\mathbf{CO_2H/NH_2}$ and **CDs**–$\mathbf{CO_2H}$ cells, suggesting that these nanoparticles are not accumulated within *C. albicans* cells. Conversely, almost all cells exhibited a slight fluorescent signal after about 5 min of **CDs**–$\mathbf{NH_2}$

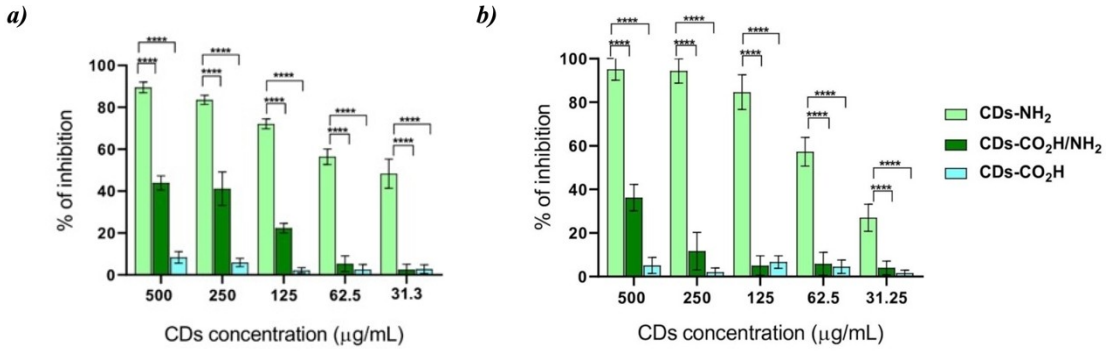

Figure 5. Inhibition of *C. albicans* ATCC 10231 24 h (a) and 48 h (b) biofilm formation in the presence of **CDs**–$\mathbf{NH_2}$ (lime green), **CDs**–$\mathbf{CO_2H/NH_2}$ (green), **CDs**–$\mathbf{CO_2H}$ (blue).

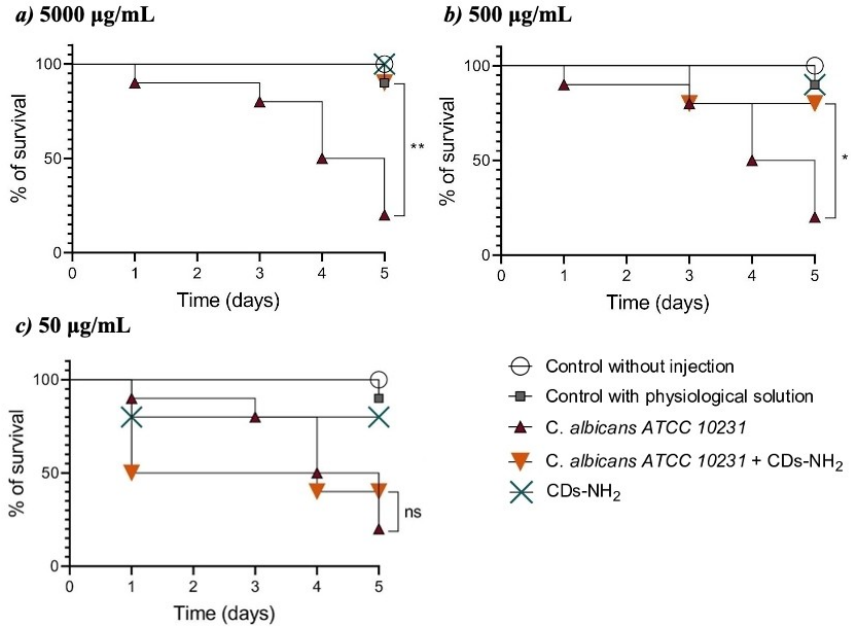

Figure 6. *G. mellonella* larvae survival rate after *C. albicans* infection and treatment with 5000 μg/mL (***a***), 500 μg/mL (***b***), 50 μg/mL (***c***) of **CDs–NH_2**.

administration. These results are comparable to the ones observed for COS-7 cells internalization, evidencing how the surface polarization dramatically influences the cell membrane interaction even in different cell types. A stronger signal was detected on the surface of the cell membrane and inside the cells after 5–10 min, suggesting that **CDs–NH_2** were accumulated on the cells at higher concentrations than in the external environment. The presence of a region, presumably corresponding to the vacuole, devoid of fluorescence was evident in cells that had internalized **CD–NH_2**, suggesting that they cannot cross the tonoplast. Since the only internalized set of CDs also is the only one active against *C. albicans* biofilm formation, it is plausible that the mechanism of inhibition could be correlated to the presence of carbon nanodots either within the cell or in the intermembrane portion.

Conclusions

In conclusion, in this work the synthesis and complete physico-chemical characterization of structurally diverse carbon nanodots was developed, with a comprehensive analysis of their biological properties as promising antifungal nanomaterials against *C. albicans* biofilm formation and adhesion. The data presented here highlight how the surface structure and the consequent polarization result crucial for the interaction with biological membranes, CDs internalization, and most importantly to exert the antifungal activity. All the developed nanodots possess good biocompatibility and extremely high cell viability even at high concentrations (up to 4.0 mg/mL) in MTT analyses with fibroblast-like COS-7 cells. Positively-polarized carbon nanodots showed internalization in COS-7 cell membrane as well as into planktonic *C. albicans* cells, observed by fluorescence microscopy analyses employing CDs intrinsic photoluminescence. The images evidence that the CDs adhere and enter *C. albicans* cells. These features are paired with a significant dose-responsive inhibition of *C. albicans* biofilm formation and adhesion, as demonstrated by *in vitro* tests, highlighting a correlation between adhesion, internalization and antifungal action. Moreover, *in vivo* tests with *G. mellonella* larvae exhibited 90% survival of larvae infected with *C. albicans* upon treatment with positively charged CDs. We believe that this study could serve as a starting point to fully explore the discovered antifungal potentialities and promising applications of carbon nanodots, so far only preliminary studied, to thoroughly clarify the CDs' mechanism of action in biofilm adhesion inhibition and possibly to employ their ability to enter in the cell to develop innovative bioactive antifungal bioconjugates as nano-carriers of active principles.

Experimental section

General information

All the chemicals were purchased from Sigma Aldrich (Milan, Italy) in a 99% purity grade, and used without purification. Ultrapure MilliQ water was used for carbon dots synthesis and dialysis. Dialysis membrane with 100–500 Da cut-off were purchased from Sigma Aldrich. For the filtration of crude CDs solutions, Millex®-VV syringe filters with 0.1 μm pore size in PVDF (33 mm) were used.

Carbon dots synthesis

CDs–NH_2 Compound **2** (550.0 mg, 5.09 mmol) was completely dissolved in MeOH by sonication (10 min) before mixing it with **1** (1.0 g, 4.64 mmol) (**1**:**2** ratio = 1:1.1) and water to reach a final solution of water/MeOH (2:1, 30 mL total). The resulting solution was then carbonised in a microwave at 800 W for 3 min. The resulting slurry solution was diluted in MilliQ water (10 mL) and centrifuged at 4,000 rpm to remove larger particles and the supernatant was directly

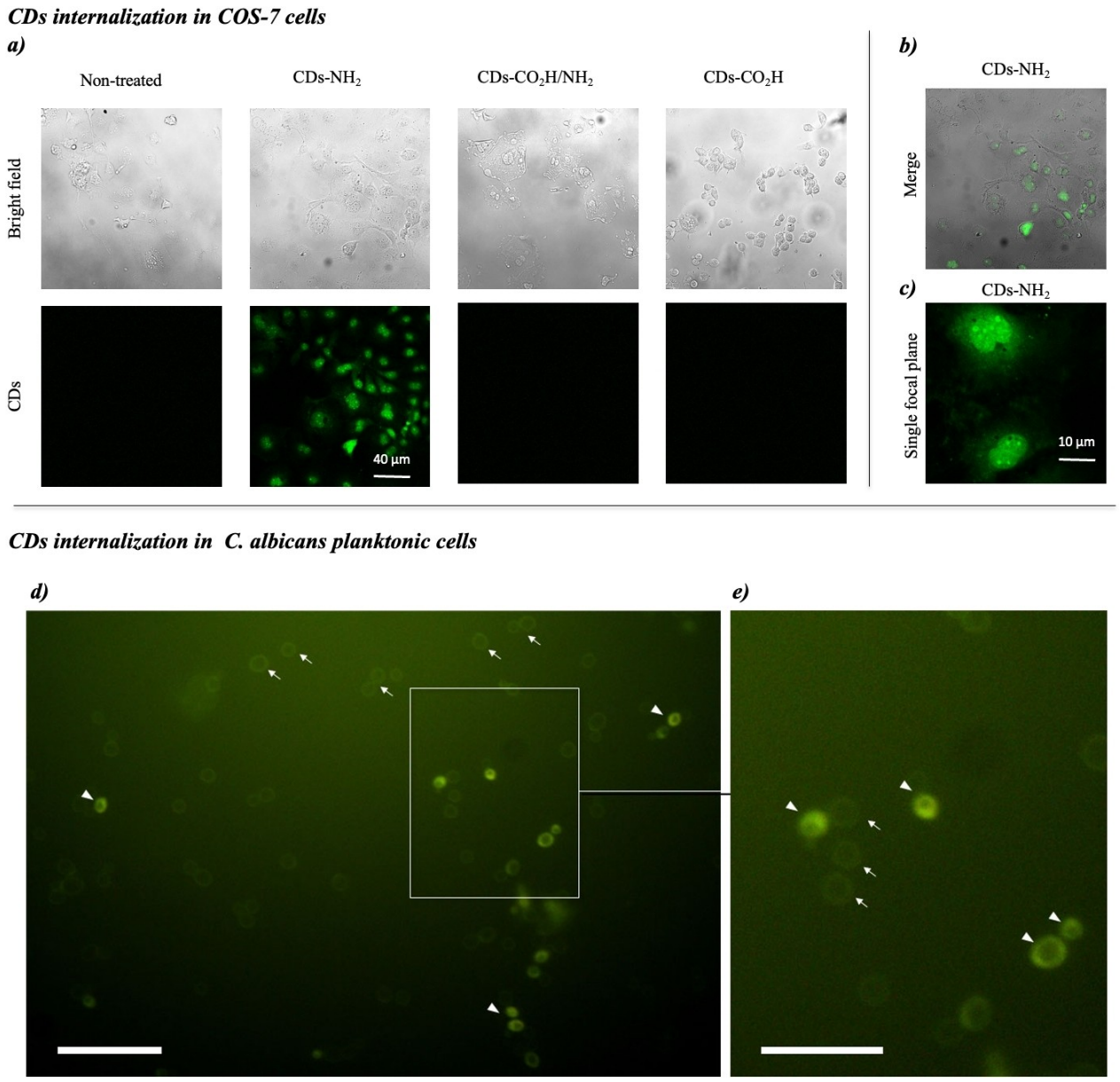

Figure 7. Confocal microscopy images for internalization studies of **CDs-NH_2**, **CDs–CO_2H/NH_2**, **CDs–CO_2H** in COS-7 cells (a, b, and c) and epifluorescence micrograph of *C. albicans* planktonic cells at the **CDs–NH_2** diffusion front (d, e). The rectangle in (d) represents the area of the detail in (e). All cells exhibit a slight fluorescence signal in the cell walls (arrows) and some of them also exhibit a more intense cytoplasmic signal (arrow heads). Bars 40 μm (a–b, d), 10 μm (c) and 5 μm (e).

dialysed for three days (dialysis water changed at least 5 times per day) and then filtered through a 100 nm syringe filter. The resulting solution was freeze-dried to obtain the desired CDs.

CDs–CO_2H/NH_2 urea (**3**) (3.0 g, 50.0 mmol) and citric acid (**4**) (2.0 g, 9.5 mmol) were dissolved in water (60 mL) at 70 °C for 15 min, followed by 20 min sonication to ensure complete solubilization. Then, the mixture was irradiated at 800 W for 30 min. The resulting slurry solution was centrifuged at 4,000 rpm to remove larger particles and the supernatant was directly dialysed for five days and then filtered through a 100 nm syringe filter. The solution was freeze-dried to obtain the desired CDs.

CDs–CO_2H D-glucose (**5**) (2.0 g, 11.1 mmol) and polyacrylate sodium (MW = 5100, **6**) (1.0 g, 0.2 mmol), in a 1:2 ratio, were dissolved in water (10 mL). The microwave-assisted carbonisation was performed via irradiation for 4 min at 800 W. The resulting slurry solution was centrifuged at 4,000 rpm to remove larger particles and the supernatant was directly dialysed for five days and then filtered through a 100 nm syringe filter. The solution was freeze-dried to obtain the desired CDs.

NMR analyses

For NMR analysis CDs were dissolved in DMSO-d_6 ar r.t. (6.0 mg/mL). NMR analyses were performed on a 300 MHz Bruker Avance III spectrometer and spectra were processed using MestReNova 6.0.2 (Mestrelab research SL). Residual internal solvent was used as standard. The ^{1}H NMR spectrum of **CDs–CO_2H** was registered in a mixture 1:1 of DMSO-d_6 and D_2O, due to low solubility of CDs in pure DMSO.

AFM

AFM measurements were carried out by a Dimension Icon (Bruker AXS) under ambient conditions, in Tapping mode by using silicon RTESP-300 Bruker probes, with nominal radius of curvature 10 nm. Freshly prepared CDs solutions at 15 mg/mL have been filtered (0.1 μm pore size) and then incubated on freshly cleaved mica for 2 min to allow CDs adsorption. Then the substrate surface was washed three times with Milli Q-water to remove non-adsorbed particles. AFM images were analyzed using Gwyddion free software. Height Sensor images were processed by flattening and background subtraction.

DLS/DELS

To measure size and electrophoretic mobility of samples, Dynamic and Dielectrophoretic light scattering (DLS, DELS) measurements have been carried out by a Malvern NanoZetaSizer apparatus (Malvern Instruments, Worcestershire, United Kingdom), with backscattering configuration (173°) equipped with a 5 mW HeNe laser ($\lambda = 632.8$ nm). Temperature is controlled by a Peltier system and it was fixed at 298 K for both measurements. The CDs solution was measured at a 15 mg/mL concentration. In DLS the G1 autocorrelation function of scattered intensity is analyzed to obtain the distribution of the diffusion coefficients D of the particles, which, in turn, are converted in a distribution of hydrodynamic radii RH using the Stokes Einstein relationship $RH = kBT/6\pi\eta D$, where kBT is the thermal energy and η the solvent viscosity. Number-weighted NNLS algorithm[23] is used to determine the size and size distribution of the CDs.

For the determination of ζ-potential, electrophoretic mobility μ was converted into ζ-potential by the Smoluchowski relation $\zeta = \mu\ \eta/\varepsilon$, where η and ε are the viscosity and the permittivity of the solvent phase, respectively.[24]

Fluorescence analyses

Fluorescence of CDs in water solution was studied using Fluoromax-3 Horiba Jobin–Yvon fluorometer at 25 °C in a range between 400 and 650 nm. UV measurements were recorded on HP DIODE ARRAY instruments between 190 and 820 nm, with 2 nm resolution. For both analysis CDs were dissolved in Milli-Q water and tested in quartz cuvettes. Infrared spectra were acquired in attenuated total reflection (ATR) using a Nicolet 6700 (Thermo Fisher Scientific, Waltham, MA, USA) equipped with a Golden Gate single reflection diamond ATR accessory. All spectra were recorded in absorption mode with 200 scans/spectrum and at 4 cm^{-1} resolution in the region between 4000 and 650 cm^{-1}.

XPS analyses

For each of the C-dots samples, a drop (50 πL, 1 mg mL^{-1}) was deposited onto a hydrogenated silicon surface and let dry overnight before measurement.

XP spectra were recorded using a modified Omicron NanoTechnology MXPS system equipped with a monochromatic source (Omicron XM-1000) and an Omicron EA-125 energy analyzer. The exciting radiation used was Al Kα ($h\upsilon = 1486.7$ eV), generated operating the anode at 14 kV and 16 mA. All photoionization regions were acquired using an analyzer pass energy of 20 eV, except for the survey scan, taken at 50 eV pass energy, and a take-off angle (θ) of 21° with respect to the sample surface normal. The measurements were performed at room temperature, and the base pressure in the analyzer chamber was about 2×10–9 mbar. Experimental data were fitted using a Shirley function to reproduce the secondary electrons' background and pseudo-Voigt functions for the elastic peaks. These curves are described by a common set of parameters (position, FWHM, Gaussian-Lorentzian ratio) which were let free to vary within narrow limits. The Gaussian-Lorentzian ratio was left free to vary between 0.7 and 0.9.

Elemental analysis

Elemental analyses for C, H, and N were provided by the "Servizio di Microanalisi" at the Dipartimento di Chimica Università "La Sapienza" (Rome) on a EA 1110 CHNS-O Carlo Erba instrument.

Cell cultures and cellular viability MTT assay

COS-7 cells (ECACC 87021302) were seeded at a density of 15,000 cells per well in a 96-well plate containing complete high-glucose DMEM medium supplemented with glutamine (20 mM) and 10% FBS. The compounds **CDs–NH_2**, **CDs–CO_2H/NH_2** and **CDs–CO_2H** were weighed under semi-sterile conditions and mechanically dissolved in Optimem medium for 24 hours at room temperature. After 24 hours, these solutions were filtered through a 0.2 μm filter, aliquoted and frozen at −20 °C. On the day of the experiment, the compounds were added to the wells starting from 4 μg/μl and performing serial 1:2 dilutions in Optimem medium directly in the wells, reaching a final concentration of 0.125 μg/μl (see Table S3). Following a 48 hour incubation, cell viability was assessed using the MTT colorimetric assay (Abcam, ab211091), following the manufacturer's protocol. Briefly, the assay involved an incubation of 1.5 hours at 37 °C, followed by lysis in acid isopropanol and measurement of the absorbance of the resulting solutions at 590 nm using a spectrophotometer (Multiscan FC, ThermoFisher). Additionally, to visualize the cell death we performed the trypan blue assay. Briefly, 500,000 cells were plated in a 6 well plate. The next day, compounds were added in the wells at 4 μg/μl. After 48 hours of incubation, the culture medium supernatant (CMS) was centrifuged at 200 g for 5' to pellet floating cells; the supernatant was discarded and cells were resuspended in 50 μl of PBS 1x. The cells in the 6 well plate were washed with PBS 1x and detached from the plate with 0.2 mL of trypsin-EDTA for 5' at 37 °C. Cells were mechanically detached adding 1 mL of PBS 1x and centrifuged at 2500 rpm for 10', the supernatant was discarded and cells were resuspended in 100 μl of PBS 1x. 10 μl of either type of cell resuspensions were mixed with 10 μl of trypan blue (1:1 proportion). 10 μl of the mix were added to a Burker counting chamber and photographed at a 10x magnification with an RS-500 C camera.

In vivo confocal microscopy imaging of the cells

15 '000 COS-7 cells were seeded on polylysine coated (Merck; 25988–63-0) glass slides in a 24 well plate and incubated for 24 hours in a complete high-glucose DMEM medium supplemented with glutamine (20 mM) and 10% FBS. The next day the compounds dissolved as above were added at 4 μg/μl to the cells and incubated for 24 hours at 37 °C. The next day, after a wash in PBS, cells were mounted on slides adding a small drop of PBS to facilitate adhesion and living cells were analysed by confocal microscopy (Zeiss 780) with 63x and 100x magnification. Multiple Z planes were acquired with an inter-plane separation of 1 μm. Bright field and carbon dots were imaged with the bright field filter and blue filter (λ_{exit} 450–490 nm; λ_{flu} 515 nm). The confocal images were processed with Image J software (Fiji).

Antifungal susceptibility testing

Candida albicans ATCC 10231 was obtained from the American Type Culture Collection (ATCC, Rockville, MD, USA). *In vitro*, the antifungal activity of the three sets of CDs (**CDs–NH_2**, **CDs–CO_2H/NH_2** and **CDs–CO_2H**) against *C. albicans* ATCC 10231 was determined according to the standardized methods for yeast, using the broth microdilution

method.[18] *C. albicans* was grown on Sabouraud dextrose agar (Sigma Aldrich, St. Louis, MO, USA) at 35 °C for 24 h. The final concentration of the inoculum was ranging from 5.0×10^2 to 2.5×10^3 cells/mL.

CDs–NH_2, **CDs–CO_2H/NH_2** and **CDs–CO_2H** were firstly dissolved in RPMI-1640 medium. Each of them was then serially diluted 2-fold in RPMI-1640 medium (Sigma-Aldrich, St Louis, MO, USA) buffered with MOPS (4-morpholinepropanesulfonic acid) in glass tubes. The tested concentrations of the three sets of CDs ranged from 500 μg/mL to 0.976 μg/mL. After incubation, the minimal inhibitory concentration (MIC) was determined. With the help of a reading mirror, it was possible to compare the growth in each well with the control one, which is drug-free. MIC_{50} was the lowest concentration that caused a prominent decrease (≥ 50 %) in visible growth compared with the drug-free control. Each experiment was performed in duplicate and was repeated at least three times on separate dates. The results are expressed as the geometric mean.

In vitro activity of CDs against C. albicans adhesion

Candida adhesion assay was conducted as described above.[20] Presterilized, polystyrene, flat bottom 48-well microtiter plates were used. At first, *C. albicans* suspension was prepared in RPMI-1640 buffered with MOPS at a concentration of 1.0×10^6 cell/mL. 200 μL aliquot of that suspension was transferred into microtiter plate wells together with the nanoparticles' solution (final concentration ranging from 500 μg/mL to 31.25 μg/mL) and the plate incubated for 90 minutes and 24 h at 37 °C.[54] After both set times had passed, the cell suspensions were aspirated, and each well was washed twice with Phosphate Buffered Saline (PBS) to remove loosely adherent cells. Thus, *Candida* adhesion was studied quantitatively at 90 minutes, using Crystal Violet (CV) assay. In short, 200 μL of CV 0.1 % solution was added to each well. After 10 minutes, the solution was aspirated, and the wells were washed with sterile water. Following the removal of CV, 200 μl of 95 % ethanol were added to each well.[21] Eventually, the colorimetric changes showing the biomass of *Candida* biofilm were measured at 590 nm using a microplate reader. The experiment was performed three times independently in triplicate, and the results were expressed as mean ± standard deviation (SD).

In vitro activity of CDs against C. albicans biofilms

The *Candida* biofilm was formed on flat-bottomed, 48-well microtiter plates, as previously described with some modifications.[19b] To evaluate the CDs' activity against the formation of biofilm, a suspension of *C. albicans* was prepared in RPMI-1640 buffered with MOPS. 200 μL aliquots of this cell suspension (final concentration in well: 1.0×10^5 cells/mL) were added to the 48 microplate wells together with 200 μL of each set of nanoparticles solution at a concentration ranging from 500 μg/mL to 31.25 μg/mL. Plates were then incubated for 24 h and 48 h at 37 °C. After biofilm formation, the medium was aspirated, and non-adherent cells were removed by washing twice with phosphate-buffered saline (PBS). *C. albicans* biomass was quantified using Crystal Violet (CV) assay as described above.[56] Eventually, the colorimetric changes showing the biomass of *Candida* biofilm were measured at 590 nm using a microplate reader. The experiment was performed three times independently in triplicate, and the results were expressed as mean ± standard deviation (SD).

Galleria mellonella survival assay

Galleria mellonella survival assays were carried out as described by Cairone and colleagues.[14d] Larvae of *G. mellonella* of 0.3 ± 0.03 g, obtained from Todaro Sport (Rome, Italy), were selected. Nine groups of larvae (10 larvae for each group, 1 group for each treatment) were inoculated in the last left proleg with 2×10^6 cells of *C. albicans* ATCC 10231 and with 10 μL of **CDs–NH_2**. The concentrations of **CDs–NH_2** were 50 mg/mL, 5 mg/mL, 0,5 mg/mL. Three groups with respectively 50 μg/larva, 5 μg/larva and 0,5 μg/larva of **CDs–NH_2** were defined to investigate **CDs–NH_2** toxicity on *G. mellonella* larvae. Three control groups were used: one group of larvae were pierced with no treatment applied, one group were treated with sterile saline solution and one group were treated with *C. albicans* ATCC 10231. The larvae were then incubated at 37 °C and monitored for 120 h. They were considered dead when they did not respond to physical stimulation (a slight pressure with forceps). Each experiment was repeated at least three times and reported as a percent survival rate.

Fungal uptake

To evaluate the CDs uptake, *C. albicans* was cultured on Sabouraud dextrose agar (Sigma Aldrich, St. Louis, MO, USA) at 35 °C for 24 h. After that time, a suspension in SDB at a final concentration of 1×10^4 conidia/mL was obtained and cultured on glass microscope slides placed into Petri dishes previously filled with 5 mL sterile SDB and incubated for additional 24 h. 200 μL of CDs at a final concentration of 1 mg/mL were added to the edge of the coverslip placed over the biofilm in formation and fungal uptake was observed over time under a fluorescence microscope (Leica DMRB) equipped with blue filter (λ_{exit} 450–490 nm; λ_{flu} 515 nm). The control of untreated cells was observed to reveal any auto-fluorescence. The experiments were repeated three times independently.

Supporting Information

The Supporting Information is available free of charge on the ACS Publications website: NMR, DLS/DELS, AFM, UV-Vis, IR, and XPS spectra, elementar analysis, MTT and antifungal assays, cell uptake.

Author Contributions

The manuscript was written through contributions of all authors. All authors have given approval to the final version of the manuscript. Author contribution: E. S., F. V., F. L. conceptualization, data curation, funding acquisition, investigation supervision, validation, writing original draft, writing – review & editing; A. C., V. G. M., G. B., I. S., F. A., B. S. data curation, formal analysis, investigation, methodology, writing–review & editing; G. S., A. V. E. M., A. G. M., L. M. M., S. S. data curation, formal analysis, investigation, resources, supervision, methodology, writing–review & editing.

Acknowledgements

Financial support from Sapienza University of Rome (grant number AR222181692DA18E, RM12117A81FD8EE0, and RM1221814C52ED98) is gratefully acknowledged. S. S. acknowledges CNIS–Research Center for Nanotechnology applied to Engineering of Sapienza, Sapienza University, Rome for access to AFM instrument.

Conflict of Interests

The authors declare no conflict of interest.

Data Availability Statement

The data that support the findings of this study are available in the supplementary material of this article.

Keywords: antiadhesion · antibiofilm · antifungal · bioactive nanomaterials · carbon dots

[1] a) Z. Kang, S.-T. Lee, *Nanoscale* **2019**, *11*, 19214–19224; b) M. Li, T. Chen, J. J. Gooding, J. Liu, *ACS Sens.* **2019**, *4*, 1732–1748; c) X. Wang, Y. Feng, P. Dong, J. Huang, *Front. Chem.* **2019**, *7*; d) Y. Park, Y. Kim, H. Chang, S. Won, H. Kim, W. Kwon, *J. Mater. Chem. B* **2020**; e) L. Cui, X. Ren, M. Sun, H. Liu, L. Xia, *Nanomaterials* **2021**, *11*, 3419.

[2] a) D. Rocco, V. G. Moldoveanu, M. Feroci, M. Bortolami, F. Vetica, *ChemElectroChem* **2023**, *n/a*, e202201104; b) X. Ding, Y. Niu, G. Zhang, Y. Xu, J. Li, *Chem. Asian J.* **2020**, *15*, 1214–1224.

[3] a) T. C. Wareing, P. Gentile, A. N. Phan, *ACS Nano* **2021**, *15*, 15471–15501; b) C. Kang, Y. Huang, H. Yang, X. F. Yan, Z. P. Chen, *Nanomaterials* **2020**, *10*, 2316.

[4] L. Đorđević, F. Arcudi, M. Cacioppo, M. Prato, *Nat. Nanotechnol.* **2022**, *17*, 112–130.

[5] a) H. Yan, M. Cacioppo, S. Megahed, F. Arcudi, L. Đorđević, D. Zhu, F. Schulz, M. Prato, W. J. Parak, N. Feliu, *Nat. Commun.* **2021**, *12*, 7208; b) T. C. Canevari, M. Nakamura, F. H. Cincotto, F. M. de Melo, H. E. Toma, *Electrochim. Acta* **2016**, *209*, 464–470; c) S. Pramanik, S. Chatterjee, G. Suresh Kumar, P. Sujatha Devi, *Phys. Chem. Chem. Phys.* **2018**, *20*, 20476–20488; d) A. Sharma, J. Das, *J. Nanobiotech.* **2019**, *17*, 92.

[6] Y. Li, Z. Tang, Z. Pan, R. Wang, X. Wang, P. Zhao, M. Liu, Y. Zhu, C. Liu, W. Wang, Q. Liang, J. Gao, Y. Yu, Z. Li, B. Lei, J. Sun, *ACS Nano* **2022**, *16*, 4357–4370.

[7] a) G. Filippini, F. Amato, C. Rosso, G. Ragazzon, A. Vega-Peñaloza, X. Companyó, L. Dell'Amico, M. Bonchio, M. Prato, *Chem.* **2020**, *6*, 3022–3037; b) V. Corti, B. Bartolomei, M. Mamone, G. Gentile, M. Prato, G. Filippini, *Eur. J. Org. Chem.* **2022**, *2022*, e202200879; c) M. Bortolami, I. I. Bogles, C. Bombelli, F. Pandolfi, M. Feroci, F. Vetica, *Molecules* **2022**, *27*, 5150; d) S. Liu, Y. He, Y. Liu, S. Wang, Y. Jian, B. Li, C. Xu, *Chem. Commun.* **2021**, *57*, 3680–3683; e) F. Arcudi, L. Dordevic, M. Prato, *Angew. Chem. Int. Ed.* **2016**, *55*, 2107–2112; f) L. Đorđević, F. Arcudi, A. D'Urso, M. Cacioppo, N. Micali, T. Bürgi, R. Purrello, M. Prato, *Nat. Commun.* **2018**, *9*, 3442; g) C. Rosso, G. Filippini, M. Prato, *ACS Catal.* **2020**, *10*, 8090–8105; h) G. Gentile, M. Mamone, C. Rosso, F. Amato, C. Lanfrit, G. Filippini, M. Prato, *ChemSusChem.* **2023**, e202202399; i) C. Michenzi, C. Espro, V. Bressi, C. Celesti, F. Vetica, C. Salvitti, I. Chiarotto, *J. Mol. Catal.* **2023**, *544*, 113182.

[8] a) F. Lin, Z. Wang, F.-G. Wu, *Pharmaceuticals* **2022**, *15*, 1236; b) Z.-X. Wang, Z. Wang, F.-G. Wu, *ChemMedChem* **2022**, *17*, e202200003.

[9] a) R. Jijie, A. Barras, J. Bouckaert, N. Dumitrascu, S. Szunerits, R. Boukherroub, *Colloids Surf. B.* **2018**, *170*, 347–354; b) M. Ghirardello, J. Ramos-Soriano, M. C. Galan, *Nanomaterials* **2021**, *11*, 1877–1901; c) P. Ezati, J.-W. Rhim, R. Molaei, R. Priyadarshi, S. Roy, S. Min, Y. H. Kim, S.-G. Lee, S. Han, *Sustainable Materials and Technologies* **2022**, *32*, e00397.

[10] a) Y. Chen, Y. Gao, Y. Chen, L. Liu, A. Mo, Q. Peng, *J. Controlled Release* **2020**, *328*, 251–262; b) W. Bing, H. Sun, Z. Yan, J. Ren, X. Qu, *Small* **2016**, *12*, 4713–4718; c) A. Saravanan, M. Maruthapandi, P. Das, S. Ganguly, S. Margel, J. H. T. Luong, A. Gedanken, *ACS Applied Bio Materials* **2020**, *3*, 8023–8031; d) J. Yang, X. Zhang, Y.-H. Ma, G. Gao, X. Chen, H.-R. Jia, Y.-H. Li, Z. Chen, F.-G. Wu, *ACS Appl. Mater. Interfaces* **2016**, *8*, 32170–32181; e) J. Zhang, X. Lu, D. Tang, S. Wu, X. Hou, J. Liu, P. Wu, *ACS Appl. Mater. Interfaces* **2018**, *10*, 40808–40814; f) N. Xu, J. Du, Q. Yao, H. Ge, H. Li, F. Xu, F. Gao, L. Xian, J. Fan, X. Peng, *Carbon* **2020**, *159*, 74–82.

[11] K. Kostov, B. Andonova-Lilova, G. Smagghe, *Biotechnol. Biotechnol. Equip.* **2022**, *36*, 949–959.

[12] a) D. C. de Moraes, *Journal of Medical Mycology* **2022**, *32*, 101232; b) A. Logan, A. Wolfe, J. C. Williamson, *Current Infectious Disease Reports* **2022**, *24*, 105–116.

[13] E. Butassi, L. Svetaz, M. C. Carpinella, T. Efferth, S. Zacchino, *Antibiotics* **2021**, *10*, 1053.

[14] a) G. De Angelis, G. Simonetti, L. Chronopoulou, A. Orekhova, C. Badiali, V. Petruccelli, F. Portoghesi, S. D'Angeli, E. Brasili, G. Pasqua, C. Palocci, *Sci. Rep.* **2022**, *12*, 7989; b) M. Bortolami, F. Pandolfi, A. Messore, D. Rocco, M. Feroci, R. Di Santo, D. De Vita, R. Costi, P. Cascarino, G. Simonetti, L. Scipione, *Bioorg. Med. Chem. Lett.* **2021**, *42*, 128087; c) D. De Vita, A. Messore, C. Toniolo, C. Frezza, L. Scipione, C. M. Bertea, M. Micera, V. Di Sarno, V. N. Madia, I. Pindinello, P. Roscilli, A. Botto, G. Simonetti, A. Orekhova, S. Manfredini, R. Costi, R. Di Santo, *Nat. Prod. Res.* **2021**, *35*, 4621–4626; d) F. Cairone, G. Simonetti, A. Orekhova, M. A. Casadei, G. Zengin, S. Cesa, *Molecules* **2021**, *26*, 1731; e) M. Di Consiglio, E. Sturabotti, B. Brugnoli, A. Piozzi, L. M. Migneco, I. Francolini, *Polym. Chem.* **2023**, *14*, 432–442; f) E. Sturabotti, V. G. Moldoveanu, A. Camilli, A. Valletta, G. Simonetti, E. Miranda, L. M. Migneco, A. Martinelli, F. Vetica, F. Leonelli, *ACS Macro Lett.* **2023**, 1079–1084; g) F. Leonelli, A. La Bella, A. Francescangeli, R. Joudioux, A.-L. Capodilupo, M. Quagliariello, L. M. Migneco, R. M. Bettolo, V. Crescenzi, G. De Luca, D. Renier, *Helv. Chim. Acta* **2005**, *88*, 154–159.

[15] S. A. Hill, S. Sheikh, Q. Zhang, L. Sueiro Ballesteros, A. Herman, S. A. Davis, D. J. Morgan, M. Berry, D. Benito-Alifonso, M. C. Galan, *Nanoscale Adv.* **2019**, *1*, 2840–2846.

[16] H. Sutanto, I. Alkian, N. Romanda, I. W. L. Lewa, I. Marhaendrajaya, P. Triadyaksa, *AIP Adv.* **2020**, *10*, 055008.

[17] Q. Liu, S. Xu, C. Niu, M. Li, D. He, Z. Lu, L. Ma, N. Na, F. Huang, H. Jiang, J. Ouyang, *Biosens. Bioelectron.* **2015**, *64*, 119–125.

[18] a) *Reference Method for Broth Dilution Antifungal Susceptibility Testing of Yeasts*, 3rd ed. Approved Standard. CLSI M27-A3(28), Clinical and Laboratory Standards Institute, Wayne, PA, USA, **2008**; b) Reference Method for Broth Dilution Antifungal Susceptibility Testing of Yeasts–Fourth Informational Supplement, Document M27-A3, Clinical and Laboratory Standards Institute, Wayne, PA, USA, **2012**.

[19] a) G. Simonetti, C. Passariello, D. Rotili, A. Mai, E. Garaci, A. T. Palamara, *FEMS Yeast Res.* **2007**, *7*, 1371–1380; b) A. Ourabah, D. Atmani-Kilani, N. Debbache-Benaida, O. Kolesova, L. Azib, F. Yous, M. Benloukil, B. Botta, D. Atmani, G. Simonetti, *J. Herb. Med.* **2020**, *20*, 100319.

[20] a) H. M. H. N. Bandara, B. P. K. Cheung, R. M. Watt, L. J. Jin, L. P. Samaranayake, *J. Investig. Clin. Dent.* **2013**, *4*, 186–199; b) V. H. Matsubara, Y. Wang, H. M. H. N. Bandara, M. P. A. Mayer, L. P. Samaranayake, *Appl. Microbiol. Biotechnol.* **2016**, *100*, 6415–6426.

[21] C. G. Pierce, A. K. Chaturvedi, A. L. Lazzell, A. T. Powell, S. P. Saville, S. F. McHardy, J. L. Lopez-Ribot, *npj Biofilms and Microbiomes* **2015**, *1*, 15012.

[22] I. Serrano, C. Verdial, L. Tavares, M. Oliveira, *Antibiotics* **2023**, *12*, 505.

[23] C. L. Lawson, R. J. Hanson, *Solving Least Squares Problems* Prentice-Hall, Inc., Englewood Cliffs, **1974**.

[24] R. J. Hunter, *Zeta Potential in Colloid Science: Principles and Applications* Academic Press, Cambridge, MA, USA, **2013**.

Manuscript received: November 3, 2023
Accepted manuscript online: December 7, 2023
Version of record online: ■■, ■■

RESEARCH ARTICLE

Three classes of Carbon Dots with different composition and charged surfaces were prepared and completely characterised with regards to their morphology and physicochemical properties. We demonstrate the requirement of a positively-charged surface to exert antibiofilm formation by *C. albicans* paired with anti-adhesion and internalization properties, and with a mortality reduction of infected larvae in *in vivo* tests.

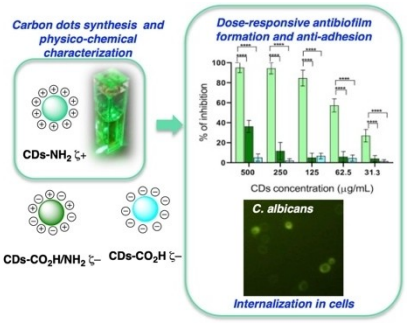

Dr. E. Sturabotti, A. Camilli, V. Georgian Moldoveanu, G. Bonincontro, Prof. Dr. G. Simonetti, Prof. Dr. A. Valletta, Dr. I. Serangeli, Prof. Dr. E. Miranda, Dr. F. Amato, Prof. Dr. A. Giacomo Marrani, Dr. L. M. Migneco, Dr. S. Sennato, Dr. B. Simonis, Dr. F. Vetica*, Prof. Dr. F. Leonelli**

1 – 12

Targeting the Antifungal Activity of Carbon Dots against *Candida albicans* Biofilm Formation by Tailoring Their Surface Functional Groups